Research Article

Preparation of Nitrogen-Doped Carbon Materials from Monosodium Glutamate and Application in Reduction of *p*-Nitrophenol

Ke Ying Cai*, Ying Mei Zhou, Peng Wang, Huan Li, Yan Li, Wei Tao

School of Chemistry and Chemical Engineering, Xuzhou University of Technology, Xuzhou, Jiangsu 221018, China

Abstract

Nitrogen-doped carbons (NCs) as supports for metal catalysts used in heterogeneous reactions are increasingly being investigated. In this work, NCs were prepared from monosodium glutamate (MSG) by direct carbonization, which were used as supporters to prepare Bi/NC catalysts. The Bi/NC catalysts were characterized by X-ray powder diffraction (XRD), X-ray photoelectron spectroscopy (XPS), transmission electron microscope (TEM), and nitrogen adsorption isotherm. The results indicate that nitrogen was doped in the formation of pyridinic N, pyrrolic N, and graphitic N. The NCs possess high surface area (~652 m²/g) and uniform mesopore size (~2.11 nm). Bismuth nanoparticles (NPs) dispersed uniformly in NC with diameter of 10-20 nm. The catalytic performances were investigated using the reduction of 4-nitrophenol (4-NP) with excess potassium borohydride as a model reaction, the results indicating that the Bi/NC catalysts have higher activity and better reusability than the Bi/AC catalyst. Under the following conditions: 100 mL of 4-NP (2 mM), 0.03 g of 3%Bi/NC, $n(KBH_4) : n(4\text{-}NP) = 40:1$, and at room temperature, the rate constant k can reach 0.31 min^{-1}. Copyright © 2018 BCREC Group. All rights reserved

Keywords: Reduction; 4-Nitrophenol; Nitrogen-doped carbon; Monosodium glutamate

1. Introduction

Carbon materials have attracted more and more attention owing to their broad availability, environmental acceptability, corrosion resistance, and unique surface properties [1]. All these aspects make carbon materials promising for various application, including energy conversion and storage, electrocatalysis, heterogeneous catalysis, and sensors. Other than morphology control, chemical doping is another important approach to modify the property of carbon materials, which has been demonstrated as a successful method to tune carbon's electronic structure, increasing active sites and enhancing catalytic activity significantly [2]. Of all the alternative dopant elements, the nitrogen-involved modification has attracted much atten-

---

* Corresponding Author.
   E-mail: caikeying@163.com (Cai, K.Y.)
   Telp.: +86-13852081673; Fax.: +86-516-85608300

tion because the charge distribution of carbon atoms will be influenced by the neighbor nitrogen atoms [3]. Thus nitrogen-doped carbon (NC) has different properties compared with the pristine carbon, which broaden its applications [4]. For instance, NC activated by doped nitrogen can be used as a catalyst in oxygen reduction reaction (ORR) [5,6] and heterogeneous catalytic reactions [2]. NC can also be used as a catalyst carrier in some heterogeneous catalytic reactions, which can anchor the metal NPs firmly [7]. Moreover, NCs can be used in batteries, sensors, and ultracapacitors [4].

NC can be obtained through two different ways: direct synthesis and post treatment. Direct synthesis includes chemical vapor deposition (CVD), segregation growth, solvothermal, and arc-discharge approaches. Post treatment includes thermal treatment, plasma treatment, and N_2H_4 treatment [1]. The main shortcoming of post treatment is that it entails numerous synthetic steps, hence direct synthesis is more commonly utilized in the synthesis of NC [8]. Furthermore, nitrogen distribution can be more uniform in carbon material by direction synthesis. Many substances can be used as precursors for NC materials by direct synthesis such as gelatin [9], chitosan [10], pyrrole [11], dopamine [12], and aniline [13].

Monosodium glutamate (MSG) with amino group is a kind of perfect raw material for NC, because it is inexpensive and easy to obtain. To the best of our knowledge, few NC materials from MSG were studied. Yan and co-workers synthesized porous carbon nanoflakes by cooking a mixture of MSG and sodium chloride, and the material can facilitate persistent and fast ion transport and shorten diffusion pathways for high-performance supercapacitor applications [14]. But there is no report on NC from MSG used as a metal catalyst support.

In this work, NC was synthesized by pyrolysis of MSG which was employed as a source of carbon and nitrogen. Then the as-synthesized NC was used as a support to prepare Bi/NC catalyst. The catalytic performances of Bi/NC

catalyst were investigated using the reduction of *p*-nitrophenol (4-NP) to *p*-aminophenol (4-AP) as a model reaction under mild conditions (Scheme 1). The 4-NP threatens seriously human health and natural environment due to its structural stability, difficult degradation, and water solubility, which are from the production of pesticides, herbicides, insecticides and synthetic dyes cause serious pollution [15]. But the reduced product 4-AP is less poisonous and more easily degradable than 4-NP. It is therefore necessary to develop sustainable and active catalyst for the reduction of 4-NP. Nobel metals, such as: Pd [16], Au [17], Ag [18], etc., are often used as active components in the catalysts for the reduction.

Compared with noble metals, bismuth is cheap and easily fabricated by reduction with reducing agent such as sodium borohydride and hydrazine hydrate. More importantly, bismuth is a kind of environment-friendly element. Bismuth (III) salts are considered safe and non-toxic probably due to their insolubility in neutral aqueous solutions [19]. Therefore, bismuth and its salts appeared as suitable regents for design of "eco-friendly catalyst" for the reduction of 4-NP.

2. Materials and Methods

2.1 Materials

Bismuth nitrate pentahydrate, MSG, potassium hydroxide, and 4-NP were purchased from Tianjin Fuchen Reagent Co. Ltd. (China). Potassium borohydride (95 %) was purchased from Sinopharm Chemical Reagent Co. Ltd. (China). All reagents were of analytic grade and used without further purification. Ultrapure water was used throughout the whole experiment.

2.2 Catalyst preparation

NC was synthesized by pyrolysis of MSG. Typically, 5.0 g of MSG and 1.0 g of KOH were carbonized in a horizontal tube furnace at a
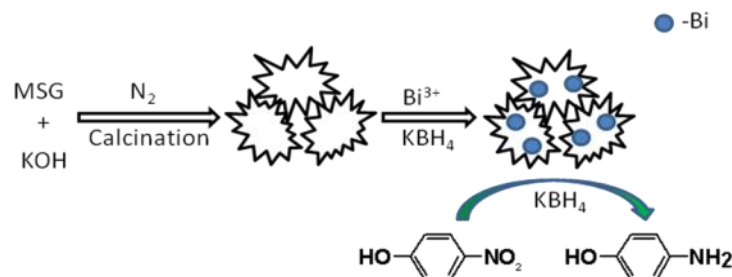
Scheme 1. Schematic illustration of the synthesis process of the Bi/NC

rate of 3 °C·min^{-1} under nitrogen flow at 700 °C for 2 h and then cooled to room temperature spontaneously. The obtained substance was washed two times with HCl (10 wt %) to remove inorganic salts, thoroughly washed with abundant water, and then dried at 100 °C for 2 h, which was denoted as NC. Bismuth nitrate pentahydrate (0.07 g) was dissolved in 5 mL of dilute nitric acid at room temperature. After bismuth nitrate dissolved completely, 15 mL of water was added and stirred. Subsequently, 1 g of NC was added to the solution and sonicated for 30 min to disperse them. Following that, 10 mL of potassium borohydride (0.5 M) solution was dropped into the mixture and stirred constantly for 1 h.

The mixture was filtered, and the obtained solids were washed with water to neutral and dried at 80 °C for 4 h. In the composite, the Bi content was about 3 %, hence the as-prepared composite denoted as 3%Bi/NC. The composites with different Bi content, such as 1%Bi/NC and 5%Bi/NC were prepared using the same method. For the purpose of comparison, activated carbon (AC) as a carrier, the 3%Bi/AC was also prepared using the same method.

2.3 Catalyst characterization

The X-ray diffraction (XRD) patterns were recorded on a diffractometer (Rigaku Ultima IV) equipped with a Cu-K$_\alpha$ radiation source. It was operated under the following conditions: tube voltage 40 kV, current 40 mA, λ = 0.15406 nm, and scanning range 2θ = 10-70°. The morphology and microstructure of the as-prepared samples were investigated with transmission electron microscope (TEM.JEOL JEM-2100). X-ray photoelectron spectroscopy (XPS) was obtained by X-ray photoelectron spectrometer (Thermo ESCALAB 250XI) using Al-Kα X-ray as the excitation source (225 W). The specific surface area of the carbons were determined in a Micromeritics sorptometer at 77 K. Before analysis, the samples were evacuated for 12 h at 250 °C under vacuum. The surface areas were calculated using the Brunauer-Emmett-Teller (BET) method based on adsorption data in the relative pressure of 0.01-0.2, and their pore diameter distributions were calculated using the Barrett-Joyner-Halenda (BJH) method.

2.4 Catalytic reduction of 4-NP

The reduction of 4-NP catalyzed by Bi/NC catalyst in the presence of an excess amount of potassium hydroxide was studied, monitored with a UV-Vis spectroscopy to examine the catalytic activity. In a typical reaction, 5 mL of 4-NP (40 mM) and 75 mL of water were mixed with 0.03 g of Bi/CN particles in a beaker at room temperature. A fresh prepared aqueous solution of 20 mL KBH$_4$ (0.4 M) was then added with constant stirring. During the reduction, the yellow color of solution gradually vanished, indicating the reduction of 4-NP. Samples were directly withdrawn from the reaction mixture at certain time intervals followed by measuring UV-Vis absorption at 400 nm. The rate constant of the reaction was determined by measuring the absorbance change in intensity at 400 nm with time.

To study the reusability of the as-prepared catalysts, the used Bi/NC catalysts were separated from the reaction solution by centrifugation after the reduction. The recycled particles were washed with ethanol and water 3 times respectively and reused. Since the absorbance is proportional to the concentration of 4-NP, the conversions were also determined by the absorbance changes of reaction solution at 400 nm [17,18].

3. Results and Discussion

3.1 Characterization of the catalysts

The phase structure of the sample was obtained through XRD measurement. As shown in Figure 1, the broad peaks located around 25° for all Bi/NC and Bi/AC samples can be index as (002) diffraction planes of the hexagonal phase graphite (JCPDS No. 41-1487) [20]. The broad pattern of diffraction peaks indicates the poor graphitization degree for all products [21]. Three diffraction peaks at approximately 27.0°, 37.8°, and 39.5° in the XRD patterns of
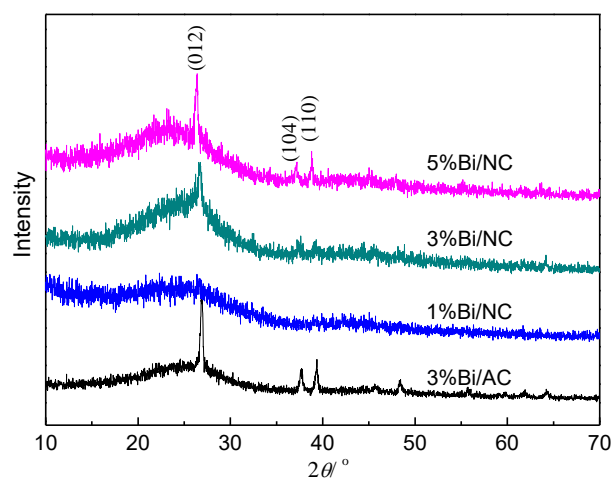

Figure 1. X-ray diffraction (XRD) patterns of the catalysts

3%Bi/NC, 5%Bi/NC, and 3%Bi/AC, can be indexed to (012), (104) and (110) planes of metallic bismuth (JCPDS No. 05-0519), respectively [22]. However, there is no the three corresponding peaks in the XRD pattern of 1%Bi/NC because of low bismuth content in it.

To determine the catalyst elemental content and the states of the N atoms, XPS was employed. As shown in Figure 2a, the XPS spectra reveal the presence of C, N, O, and Bi elements in 3%Bi/NC, but there is no N element in 3%Bi/AC. The results demonstrated that nitrogen had been successfully doped into the NC's lattice. The relative surface concentrations of C, N, O, and Bi calculated from XPS analysis were 67.86, 4.87, 27.04, and 0.23 at % in 3%Bi/NC, respectively. The N 1s spectrum (Figure 2b) can be fitted into three peaks, which can correspond to pyridinic N (398.1 eV), pyrrolic N (399.3 eV), and graphitic N (400.5 eV) [4, 23]. The N atom percent distribution in pyridinic N, pyrrolic N, and graphitic N was 30.7, 25.3, and 44.0 at %, respectively. This result indicates that the graphitic N is the main N-style in the NC catalyst. The Bi 4f spectra of the as-synthesized sampled are shown in Figure 2c. The Bi $4f^{7/2}$ and $4f^{5/2}$ peaks at approximately 160.0 eV and 165.3 eV, respectively, are considered the high-spin Bi^{3+} cation, which elucidates that bismuth oxide is the predominant bismuth phase in the targeted samples due to oxidation of bismuth particles in the air.

The structure and morphologies of 3%Bi/NC and 3%Bi/AC catalysts can be observed in the TEM images (Figure 3). The Bi particles distribute uniformly on the external surface of NC with the diameter of 10-20 nm, but the Bi particles distribute unevenly on AC with broad size distribution. The possibly reason for the result is that the Bi particles were strongly attracted by pyridinic N atoms or the carbon atoms neighboring graphitic N in NC [8,23], which can fixed Bi particles and impede them aggregation. However, there is no strong adsorption between Bi particles and AC.

The porous structure of the as-prepared materials was measured using N_2 adsorption- desorption isotherms. Figure 4a shows a type IV isotherm for 3%Bi/NC, indicating the existence of mesopores. The isotherm for 3%Bi/AC in Figure 4a exhibit a fairly sharp knee in the low relative pressure ($p/p_0 < 0.1$), which is similar to the type I curve of the microporosity characteristic. The BET surface areas of 3%Bi/NC and 3%Bi/AC are 652 m^2/g and 811 m^2/g, respectively. The pore size distribution curves were calculated by using the BJH method and are

shown in Figure 4b. Most of the pores in 3%Bi/NC are mesopores, and the average pore diameter is about 2.11 nm. However, in 3%Bi/AC most of the pores are micropores, and the average pore diameter is less than 2.0 nm.

3.2 Catalytic activity

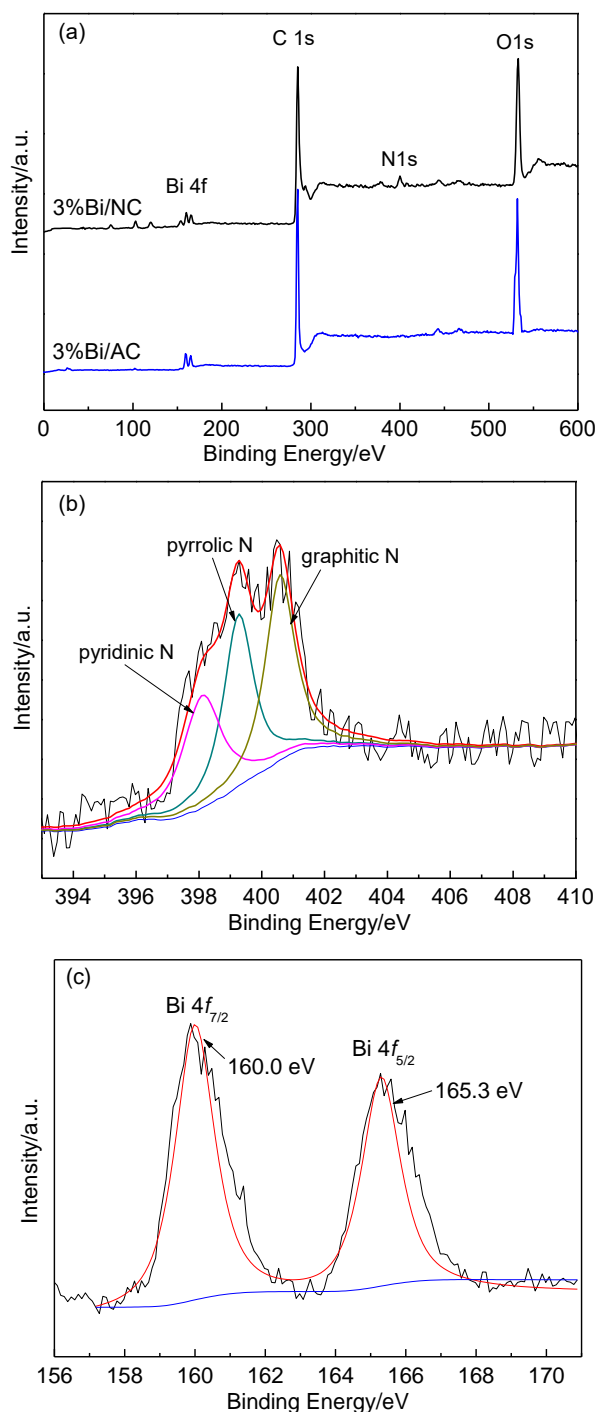To investigate the catalytic activity of the

Figure 2. XPS surveys of 3%Bi/NC and 3%Bi/AC (a), high-resolution N 1s XPS spectra (b), and high-resolution Bi 4f XPS spectra (b)

Bi/NC and Bi/AC catalysts, the reduction of 4-NP to 4-AP in the presence of excess KBH_4 was chosen as a model reaction. The reaction is particularly easy to detect because there is only one product, 4-AP, and the extent of reaction can be followed by measuring the absorbance change at 400 nm and 300 nm in UV-vis. As the concentration of KBH_4 largely exceeds the concentration of 4-NP, it can be considered as a constant during the reaction, and therefore the reduction can be regarded as pseudo-first-order reaction. Since the absorbance of 4-NP is proportional to its concentration in the medium, the ratio of A_t (t=t) to A_0 (t=0) must be equal to the concentration ratio C_t/C_0 of 4-NP [24]. The kinetic equation for the reduction can be written as Equation (1).

$$\ln(A_t/A_0)=\ln(C_t/C_0)=-kt \qquad (1)$$

In this equation k is the apparent rate constant of the reduction, which can be obtained by monitoring the decrease of the absorbance at 400 nm with time [25]. As Figure 5 shows, linear relationships of $\ln(A_t/A_0)$ versus reaction t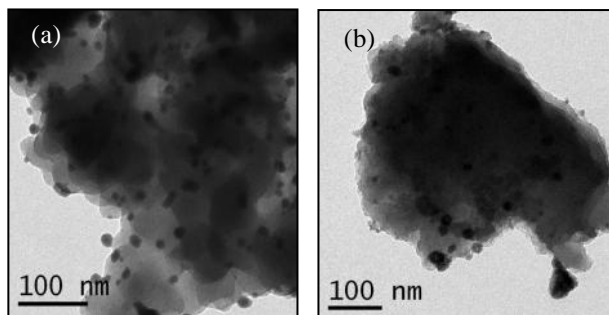ime indicate the reductions well match with pseudo-first-order, but the line slopes are different for different catalysts. The k calculated according to the line slope was 0.14, 0.19, 0.31, and 0.38 min^{-1} for 1%Bi/NC, 3%Bi/AC, 3%Bi/NC, and 5%Bi/NC, respectively. The results indicate that the catalytic activity increased with the Bi content in Bi/NC catalyst. However, when the Bi content was the same, the activity of 3%Bi/NC catalyst was higher than that of 3%Bi/AC catalyst. Since the specific surface area of 3%Bi/NC is less than that of 3%Bi/AC, it should be no contribution to the higher activity.

But the mesopores in NC can promote the transportation and reaction of reactant molecules. As shown in Figure 3, the Bi particles distribution in NC is more evenly than in AC due to the doped N atoms, so there are more active sites in NC than in AC. The result further strengthens that nitrogen doping can significantly increase metal dispersion [8].

Figure 3. TEM images of (a) 3%Bi/NC, and (b) 3%Bi/AC
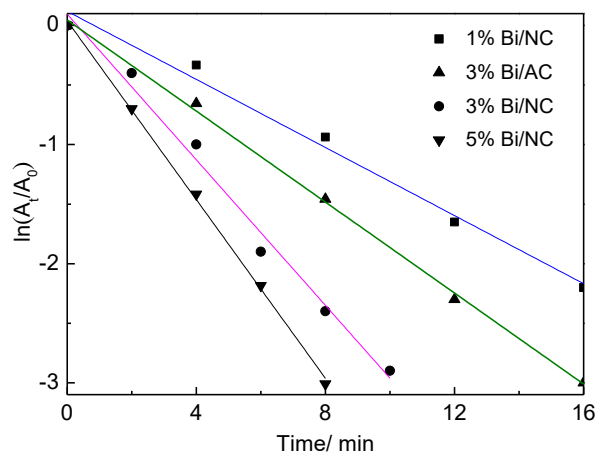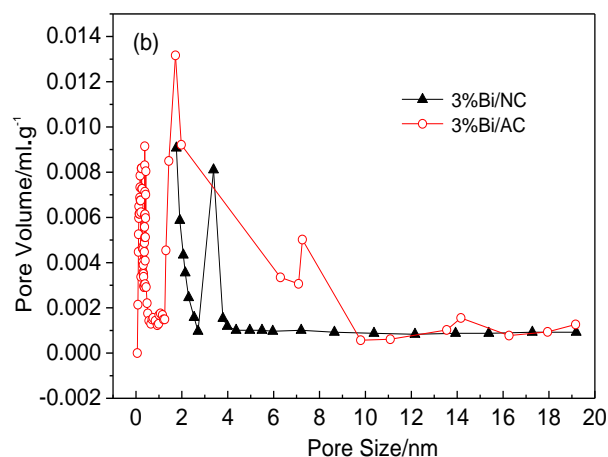

Figure 5. Activities of the catalysts

Figure 4. (a) Nitrogen adsorption-desorption isotherm and (b) pore size distribution of the catalysts

3.3 Reusability

The reusability of catalyst is of importance for practical applications. To demonstrate the reusability of the catalysts, the as-prepared catalysts were recycled by centrifugation after the reaction, washed and recycled for the reduction. As shown in Figure 6, the activity of 3%Bi/AC decreased obviously after each use, the conversion of 4-NP from 98.8 % of the first cycle to 80.5 % of the fourth cycle, but the activity of Bi/NC was more stable because of strong attraction between Bi and N atoms [23]. Since the excessive active centers may aggregate and form other less active particles, the stability was also associated with Bi content in NC, and the stability decreased with the Bi content increasing. The 1%Bi/NC, 3%Bi/NC, and 5%Bi/NC can be used for 10, 9, 6 cycles without obvious deactivation, respectively, and all of the conversions can still attained more than 97%.

4. Conclusions

In summary, the NC was prepared by carbonization of MSG and KOH, which was used as a carrier for Bi/NC catalyst. The Bi particles distribute in the NC uniformly with diameter of 10-20 nm due to the chemisorption. The catalytic performances were investigated using the reduction of 4-NP with excessive KBH_4 as a model reaction. The results indicate that the Bi/NC catalysts have higher activity and better stability than the Bi/AC catalyst. With the Bi content increasing, the activity of Bi/NC increased, but the stability decreased.

Acknowledgments

References

[1]   Zhao, Z.K., Ge, G.F., Li, W.Z., Guo, X.W., Wang, G.R. (2016). Modulating the Microstructure and Surface Chemistry of Carbocatalysts for Oxidative and Direct Dehydrogenation: A Review, *Chinese Journal of Catalysis*. 37(5): 644-670.

[2]   Kong, X.K., Chen, C.L., Chen, Q.W. (2014). Doped Graphene for Metal-free Catalysis. *Chemical Society Reviews*, 43(8): 2841-2857.
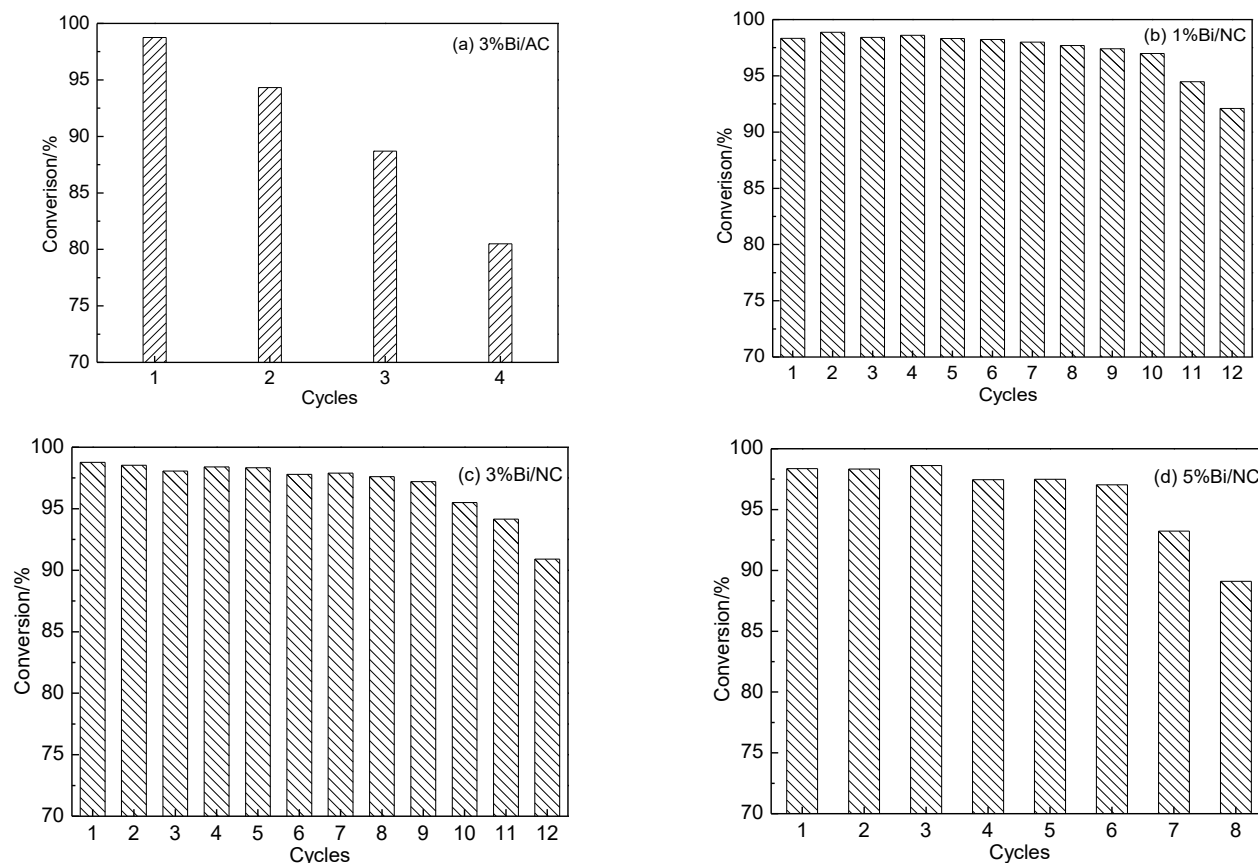

Figure 6. Reusability of the catalysts

[3] Wang, H.B., Maiyalagan, T., Wang, X. (2012). Review on Recent Progress in Nitrogen-Doped Graphene: Synthesis, Characterization, and Its Potential Applications. *ACS Catalysis*, 2(5): 781-794.

[4] Yang, Y.F., Jia, L.T., Hou, B., Li, D.B., Wang, J.G., Sun, Y.H. (2014). The Effect of Nitrogen on the Autoreduction of Cobalt Nanoparticles Supported on Nitrogen-Doped Ordered Mesoporous Carbon for the Fischer-Tropsch Synthesis. *Chemcatchem*, 6(1): 319-327.

[5] Liu, J., Song, P., Ruan, M., Xu, W. (2016). Catalytic Properties of Graphitic and Pyridinic Nitrogen Doped on Carbon Black for Oxygen Reduction Reaction. *Chinese Journal of Catalysis*, 37(7): 1119-1126.

[6] Liang, Q.Y., Su, H., Yan, J., Leung, C., Cao, S.L., Yuan, D.S. (2014). N-Doped Mesoporous Carbon as a Bifunctional Material for Oxygen Reduction Reaction and Supercapacitors. *Chinese Journal of Catalysis*, 35(7): 1078-1083.

[7] Podyacheva, O.Y., Ismagilov, Z.R. (2015). Nitrogen-doped Carbon Nanomaterials: To the Mechanism of Growth, Electrical Conductivity and Application in Catalysis. *Catalysis Today*, 249(23): 12-22.

[8] Ombaka, L.M., Ndungu, P., Nyamori, V.O. (2013). Usage of Carbon Nanotubes as Platinum and Nickel Catalyst Support in Dehydrogenation Reactions. *Catalysis Today*, 217(5): 65-75.

[9] Hu, P., Meng, D.H., Ren, G.H., Yan, R.X., Peng, X.S. (2016). Nitrogen-Doped mesoporous carbon thin film for binder-free supercapacitor. *Applied Materials Today,* 5: 1–8.

[10] Wang, Z.Q., Sun, L.X, Xu, F., Zhou, H.Y., Peng, X.J., Sun, D.L., Wang, J.C., Du, Y. (2016). Nitrogen-Doped Porous Carbons with High Performance for Hydrogen Storage. *Internal Journal of Hydrogen Energy*, 41(20): 8489-8497.

[11] Kang, W.J., Li, H.B., Ai, M., Wei, S.Y., Gao, H.Z., Liu, J.F., Qian, Y.T. (2014). Synthesis of Nitrogen-Doped Carbon and Application in Highly Selective and Sensitive Dopamine Sensing. *Materials Letters*, 116(2): 374-377.

[12] Zhang, Z., Wang, G.C., Lai, Y.Q., Li, J., Zhang, Z.Y., Chen, W. (2015). Nitrogen-Doped Porous Hollow Carbon Sphere-Decorated Separators for Advanced Lithiume-Sulfur Batteries. *Journal of Power Sources*, 300: 157-163.

[13] Niu, W.H., Li, L.G., Chen, S.W. (2017). Recent Progress in Template-Assisted Synthesis of Nitrogen-Doped Porous Carbon for Oxygen Electroreduction. *Journal of Electrochemistry*, 23(2): 110-122.

[14] Qian, W.J., Zhu, J.Y., Zhang, Y., Wu, X., Yan, F. (2015). Condiment-Derived 3D Architecture Porous Carbon for Electrochemical Supercapacitors. *Small*, 11(37): 4959-4969.

[15] Wang, Z.Z., Zhai, S.R., Zhai, B., Xiao, Z.Y., An, Q.D. (2014). Preparation and Catalytic Properties of Nano-Au Catalytic Materials Based on the Reduction of 4-Nitrophenol. *Progress in Chemistry*, 26(2/3): 234-247.

[16] Noh, J-H., Meijboom, R. (2014). Catalytic Evaluation of Dendrimer-Templated Pd Nanoparticles in the Reduction of 4-Nitrophenol Using Langmuir–Hinshelwood Kinetics. *Applied Surface Science*, 320: 400-413.

[17] Guo, P.C., Tang, L., Zeng, G.M., Huang, B.B., Dong, H.R., Zhang, Y., Zhou, Y.Y., Deng, Y.C., Ma, L.L., Tan, S.R. (2016). Catalytic Reduction-Adsorption for Removal of *p*-Nnitrophenol and Its Conversion *p*-Aminophenol from Water by Gold Nanoparticles Supported on Oxidized Mesoporous Carbon. *Journal of Colloid and Interface Science*, 469: 78-85.

[18] Li, Y.Z., Cao, Y.L., Xie, J., Jia, D.Z., Qin H.Y., Liang, Z.T. (2015). Facile Solid-State Synthesis of Ag/Graphene Oxide Nanocomposites as Highly Active and Stable Catalyst for the Reduction of 4-Nitrophenol. *Catalysis Communications*, 58: 21-25.

[19] Salvador, J.A.R., Pinto, R.M.A., Silverstre, S.M. (2009). Recent Advances of Bismuth (III) Salts in Organic Chemistry: Application to the Synthesis of Heterocycles of Pharmaceutical Interest. *Current Organic Synthesis*, 6: 426-470.

[20] Qiu, Y.Y., Yang, C.Q., Huo, J., Liu, Z.G. (2016). Synthesis of Co-N-C Immobilized on Carbon Nanotubes for Ethylbenzene Oxidation. *Journal of Molecular Catalysis A: Chemical*, 424: 276-282.

[21] Jiang, Y.Q., Chowdhury, S., Balasubramanian, R. (2017). Nitrogen-Doped Graphene Hydrogels as Potential Adsorbents and Photocatalysts for Environmental Remediation. *Chemical Engineering Journal*, 327: 751-763.

[22] Ma, D.C, Zhao, J.Z., Chu, R., Yang, S.S., Zhao, Y., Hao, X.L., Li, L.Z., Zhang, L., Lu, Y., Yu, C.Z. (2013). Novel Synthesis and Characterization of Bismuth Nano/Microcrystals with Sodium Hypophosphite as Reductant. *Advanced Powder Technology*, 24(1): 79-85.

[23] Zhao, W.L., Zhu, M.Y., Dai, B. (2017). Cobalt-Nitrogen-Activated Carbon as Catalyst in Acetylene Hydrochlorination. *Catalysis Communications*, 98: 22-25.

[24] Du, X.Y., He, J., Zhu, J., Sun, L.J., An, S.S. (2012). Ag-Deposited Silica-Coated Fe$_3$O$_4$ Magnetic Nanoparticles Catalyzed Reduction of *p*-Nitrophenol. *Applied Surface Science,* 258(7): 2717-2723.

[25] Gao, J., Jian, X., Wen, S.X., Hu, J., Liu, H.L. (2015). Plasma-Assisted Synthesis of Ag Nanoparticles Immobilized in Mesoporous Cellular Foams and Their Catalytic Properties for 4-Nitrophenol Reduction. *Microporous and Mesoporous Materials*, 207: 149-155.